

Hydrodynamic storm surge model simplification via application of land to water isopleths in coastal Louisiana



Christopher G. Siverd^{a,*}, Scott C. Hagen^{a,b,c,d}, Matthew V. Bilskie^b, DeWitt H. Braud^d, R. Hampton Peele^e, Robert R. Twilley^{d,f}

^a Department of Civil and Environmental Engineering, Louisiana State University, 257 Military Science Building, Baton Rouge, LA, 70803, United States ^b Center for Coastal Resiliency, Louisiana State University, 124C Sea Grant Building, Baton Rouge, LA, 70803, United States ^c Center for Computation and Technology, Louisiana State University, 340 E. Parker Blvd., Baton Rouge, LA, 70803, United States ^d Coastal Studies Institute, Louisiana State University, Howe-Russell Geoscience Complex, Room 331, Baton Rouge, LA, 70803, United States ^e Louisiana Geological Survey, Louisiana State University, 3079 Energy, Coast and Environment Building, Baton Rouge, LA, 70803, United States ^f College of Coast and Environment, Louisiana State University, 1002-Q Energy, Coast and Environment Building, Baton Rouge, LA, 70803, United States

ARTICLE INFO

Keywords:
Storm surge attenuation
Coastal wetland loss
Land water ratio
ADCIRC
Louisiana coastal landscape
Hydrologic unit code

ABSTRACT

The Mississippi River Delta ranks the seventh largest delta in the world. It provides a habitat for the Louisiana seafood industry, navigation canals and rivers that support five of the 15 largest cargo ports by volume in the United States, and hurricane storm surge protection for coastal cities and oil and gas industry infrastructure that facilitates 90% of the outer continental oil and gas extraction. Due to substantial coastal wetland loss since 1900, the risk of damage to these industries and infrastructure has increased through time. The goal of this research is to develop a methodology to analyze the historical and future evolution of coastal hazards, such as hurricane storm surge, across a complex, low-lying coastal landscape. To accomplish this task, the change in coastal hazards is analyzed through historical changes in coastal wetlands. Specifically, isopleths, defined as lines on a map indicating a constant value of a given variable, are developed to describe areas of constant values of the ratio of land to water (L:W) across coastal Louisiana.

In this analysis, a methodology is developed that utilizes land to water (L:W) isopleths to simplify the modern day Louisiana coastal landscape as represented in a state-of-the-art high resolution storm surge model. L:W isopleths are derived for the year 2010 and used to construct 36 storm surge models, each featuring variations of three distinct coastal zones: "High" (i.e. high wetland), "Intermediate" (i.e. wetland), and "Submersed" (i.e. region between open water and wetland). The ADvanced CIRCulation (ADCIRC) code is used to compute water surface elevations and depth-averaged currents forced by hurricane wind and pressures from Hurricanes Rita, Gustav, and Katrina for each model. Peak water levels and volume of inundation are quantified within hydrologic unit code watersheds (HUC12) in order to compare storm surge models featuring high resolution and simplified coastal landscapes.

A L:W isopleth permutation of 99%–90%–40%–1% with areas labeled "High" (99%–90%), "Intermediate" (90%–40%) and "Submersed" (40%–1%) is found to best represent simulated storm surge that most closely reproduces the high resolution storm surge model. Simulation results reveal the methodology developed in this analysis is effective in identifying an isopleth permutation that accurately simplifies a high resolution storm surge model. This result may lead to future analyses of the historical evolution of storm surge attenuation in the Mississippi River Delta (MRD) as well as other complex, low-lying deltas. These possibilities include developing storm surge models for the years 1930 and 1970, for instance, with the same isopleth permutation to examine the changes in storm surge attenuation through time. This analysis could also be applied in other similar low-lying coastal regions to conduct past and future analyses of the evolution of coastal hazards.

* Corresponding author.

E-mail addresses: csiver3@lsu.edu (C.G. Siverd), shagen@lsu.edu (S.C. Hagen), mbilsk3@lsu.edu (M.V. Bilskie), dbraud1@lsu.edu (D.H. Braud), hampton@lsu.edu (R.H. Peele), rtwilley@lsu.edu (R.R. Twilley).

1. Introduction

The wetlands of the Mississippi River Delta (MRD) comprise the seventh largest delta in the world (Couvillion et al., 2011) and create a habitat for the (approximately) USD 3 billion/year Louisiana seafood industry (Restore the Mississippi Delta Coalition, 2012). The river dominated delta (Coleman et al., 1998; Galloway, 1975) draws runoff from 31 U.S. States and two Canadian provinces (U.S. Army Corps of Engineers, 2016) and features five of the 15 largest ports (by cargo volume) in the U.S. accounting for 20% of all waterborne transport in the country (Restore the Mississippi Delta Coalition, 2012). In addition, wetlands of the MRD and of the Chenier Plain collectively comprise the Louisiana coastal landscape and provide hurricane storm surge protection for coastal cities from New Orleans to Lake Charles and oil and gas industry infrastructure that produces 90% of the U.S.'s outer continental oil and gas (Coastal Protection & Restoration Authority of Louisiana, 2017).

Unfortunately since 1900 and prior to the landfall of Hurricane Katrina in 2005, according to Costanza et al. (2008), the surface area of the MRD wetlands was reduced by 480,000 ha (1850 sq mi) and Katrina temporarily reduced the wetlands by an additional 20,000 ha (77 sq mi). This resulted in a total wetland storm protection value loss of USD 28.3 billion and USD 1.1 billion, respectively (Costanza et al., 2008). With recent studies predicting high future global and relative sea level rise (RSLR) along the Louisiana coast (Jevrejeva et al., 2016; Parris et al., 2012; Stocker et al., 2013; Sweet et al., 2017), understanding the historic response of coastal storm surge to wetland loss could provide insight into future storm surge characteristics. This understanding may also further affirm the dynamic and non-linear relationship in both space and time of RSLR and storm surge (Atkinson et al., 2012; Bilskie et al., 2014, 2016a).

In 1963, the United States Army Corps of Engineers (USACE) investigated the response of coastal storm surge to the presence of wetlands and found through observing seven storms that made landfall across coastal Louisiana that storm surge can be attenuated by approximately one vertical meter for every 14.5 horizontal kilometers of coastal wetlands (U.S. Army Corps of Engineers, 1963). However, this “rule of thumb” was derived from data with substantial scatter due to the difficulty in accounting for complex landscapes or varying hurricane characteristics (Lawler et al., 2016; Lovelace, 1994; McGee et al., 2006; Wamsley et al., 2010). Since the 1963 research by the USACE, numerous studies have employed hydrodynamic models to examine hydrodynamic coastal processes including the effect of storm parameters and local topo-bathymetry on storm surge attenuation (Barbier et al., 2013; Bunya et al., 2010; Chen et al., 2005, 2008; Chen and Zhao, 2011; Dietrich et al., 2010; Karim and Mimura, 2008; Lesser et al., 2004; Moller et al., 2014^a; Resio and Westerink, 2008; Shepard et al., 2011; Suzuki et al., 2012; van Rijn et al., 2007; Wamsley et al., 2010; Westerink et al., 2008). Storm parameters such as landfall location, wind velocity, size and duration have been shown to influence coastal storm surge propagation (Irish et al., 2008; Lawler et al., 2016; Loder et al., 2009; Resio and Westerink, 2008; Wamsley et al., 2010; Zhang et al., 2012). Furthermore, recent hydrodynamic model development studies have emphasized increasing model resolution to improve the accuracy of simulated hydrodynamic processes by better representation of coastal landscapes (Ali, 1999; Bilskie et al., 2015; Bilskie and Hagen, 2013; Blain et al., 1998; Dietrich et al., 2011; Lawler et al., 2016; Luettich and Westerink, 2004; Massey et al., 2011, 2015; Walstra et al., 2012; Westerink et al., 2008). These studies suggest that storm surge depends on the geometry of the local coastal landscape, including elevation (topography and bathymetry) and structural characteristics of the coastal vegetation (bottom roughness). Specifically, studies focused on coastal Louisiana (Loder et al., 2009; Wamsley et al., 2010) and the mid-Atlantic coastal region of the U.S. (Lawler et al., 2016) indicate that the influence of fragmented wetlands on storm surge diminishes with increased surge depth.

Finer storm surge model mesh resolution (i.e. shorter element lengths and smaller distances between mesh nodes), the application of lidar to improve topographic mapping, and advancements in high performance computing

(HPC) have clearly improved the knowledge of storm surge propagation across the coastal landscape (Bilskie et al., 2015, 2016b; Bilskie and Hagen, 2013; Bunya et al., 2010; Dietrich et al., 2010; Kashiyama et al., 1997; Massey et al., 2011; Mederos et al., 2011; Mori et al., 2014; Sanders et al., 2010). However, modern remote sensing technology, such as lidar, has only been in existence since the early 1970s. The emergence of lidar coincided with the rapid advance in computing capabilities, digital and analog electronics and later the development of global positioning systems (GPS) in the 1980s (Brock and Purkis, 2009; Krabill et al., 1984). By the 1990s, lidar technology advancement and cost reduction allowed this new technology to be deployed in the field and by the 2000s it was extensively used to map topographic features of coastal zones (Brock et al., 1999; Brock and Purkis, 2009; Sallenger et al., 1999, 2003, 2007). Lack of high-resolution elevation data for coastal wetlands and a lack of common data collection methods (i.e. airborne lidar-derived elevations versus traditional field surveys) for past decades (e.g. pre-1990) poses a challenge when attempting to model and examine storm surge response to historical coastal landscapes for historic eras (i.e. how coastal Louisiana's wetland loss over recent decades has altered storm surge attenuation and protection). Therefore, a storm surge model of the modern Louisiana coast featuring high mesh resolution and a detailed topo-bathymetric landscape cannot be compared to storm surge models developed from antiquated data (and data collection methods).

To compare storm surge response to modern and historic landscapes, an equivalent model development methodology must be employed. This can be accomplished with isolopleths describing the ratio of land to water (L:W). Isopleths have been used in fields of study such as meteorology (Sawyer, 1956) and are defined as “a line on a map connecting points at which a given variable has a specified constant value” (Merriam-Webster, 2017). In this analysis, the points of specified constant value that create a line describe the percent of land with respect to water. Presently (2017), these points can be derived from a satellite image or aerial photography to yield the constant value of the ratio of land to water along the Louisiana coast. Alternatively, the same procedure can be applied to digitized historical maps. In the present analysis, the major goal is to develop a methodology that utilizes L:W isolopleths to simplify the modern day Louisiana coastal landscape as represented in a state-of-the-art high resolution storm surge model. It is hypothesized that simulated peak water levels and inundation volume from the L:W isolopleth derived storm surge model will be comparable to that of the high resolution model. The following sections present the methodology developed to apply the L:W isolopleths to a high resolution model of coastal Louisiana, simplify it, and validate this simplified coastal landscape model by comparing it to the high resolution model.

2. Study area

The study area is the coastal Louisiana landscape bounded by the Sabine River (west), Pearl River (east), Intracoastal Waterway (ICWW) (north) and the Gulf of Mexico (south) (Fig. 1a). Within this region exists two distinct coastal landscapes; the retrograding Mississippi River Delta (MRD) (Bentley et al., 2016; Blum and Roberts, 2009) east of the Atchafalaya Delta (Fig. 1a) and the prograding Chenier Plain west of the Atchafalaya Delta (Bentley et al., 2016; Huh et al., 2001). MRD formation began approximately 7500 years before present (BP) with the substantial reduction in the rate of sea level rise (SLR) and the building of the Maringouin-Sale-Cypremort Delta southeast of the modern-day city of Lafayette. Approximately 5500 years BP the Mississippi River avulsed to begin the formation of the Teche Delta, next the St. Bernard Delta 4000 years BP, the Lafourche Delta 2500 years BP, Balize Delta 1000 years BP and the Atchafalaya-Wax Lake Deltas 400 years BP. The Balize and Atchafalaya-Wax Lake Deltas are the only two deltas still active (Bentley et al., 2016; Blum and Roberts, 2009; Roberts, 1997). The landscape formed by this process of river avulsion and delta creation is characterized by vast expanses of low elevation barrier islands, coastal marshes and forests. Following the

implementation of flood control levees along the Mississippi River, the MRD has experienced landward transgression of the Gulf of Mexico (Bentley et al., 2016; Blum and Roberts, 2009; Twilley et al., 2016).

The Chenier Plain (CP), named after a French term for oak trees, refers to a series of sea shell and sand ridges with oak trees as the predominate vegetation type. These ridges span east-west between the Atchafalaya-Wax Lake Deltas and the Sabine River with fresh and brackish marsh between each ridge (Bentley et al., 2016; Howe et al., 1935; Russell and Howe, 1935). Gould and McFarlan (1959) confirmed the ridges formed when the Mississippi River created deltas on the far eastern side of the MRD which lead to erosion in the CP. Gould and McFarlan (1959) also stated the mudflats and marshland between the Chenier ridges formed during eras of delta progradation on the west side of the MRD. Due to the currently active

Atchafalaya-Wax Lake Deltas on the west side of the MRD, the CP is in a current state of progradation (Bentley et al., 2016; Huh et al., 2001).

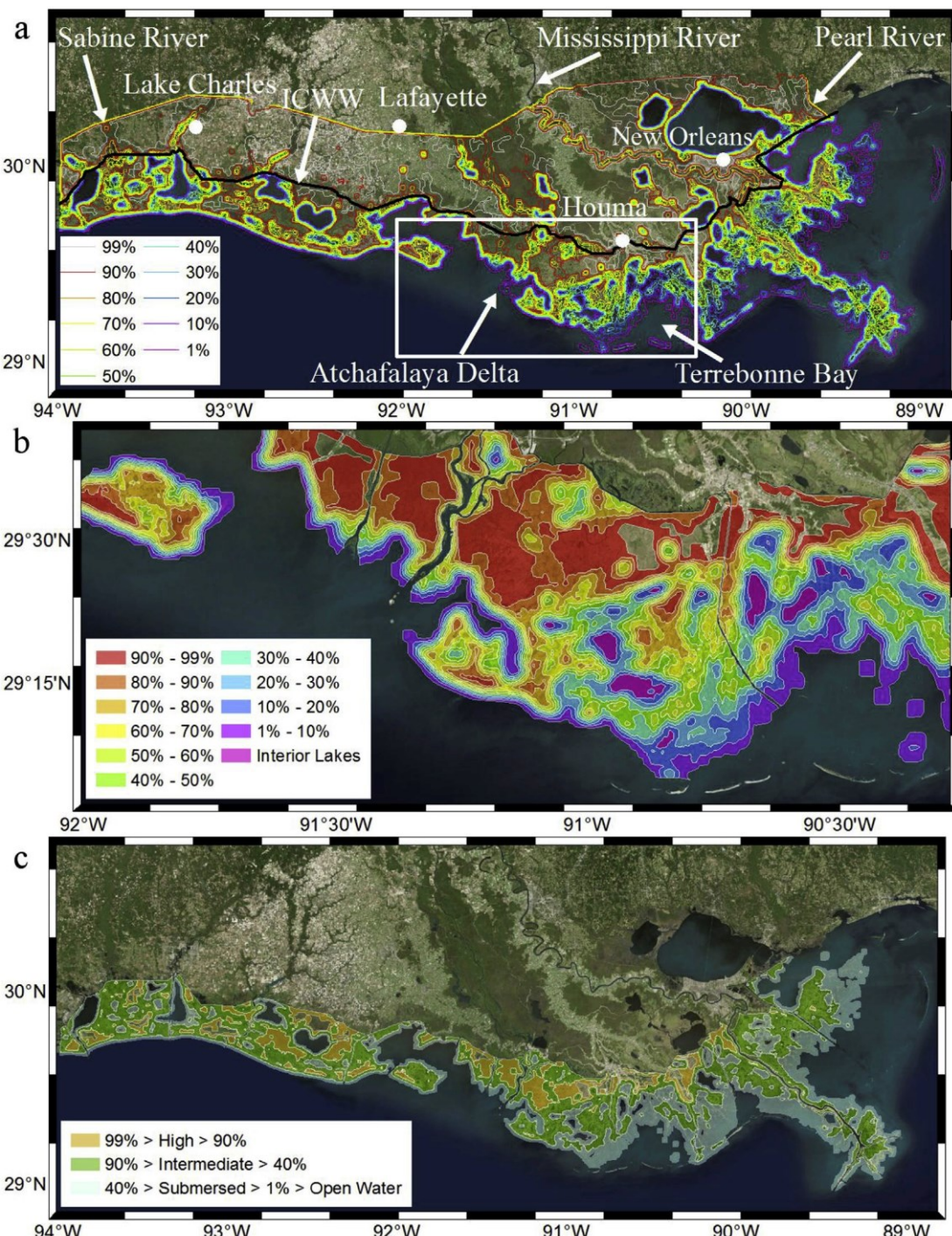


Fig. 1. a) 2010 land to water (L:W) isopleths. The black line indicates the Intracoastal Waterway (ICWW) which is the northern most boundary of this study. b) Inset from (a). Bands derived from L:W isopleths (unchanged from the detailed model: waterways, barrier islands and interior land forms). Cool colors indicate bands with more water than land. Warm colors indicate bands with more land than water. c) 2010 polygons derived from the bands in (b) for isopleth permutation 99%–90%–40%–1%. (For interpretation of the references to color in this figure legend, the reader is referred to the Web version of this article.)

3. Hydrodynamic model

The ADvanced CIRCulation (ADCIRC) code is utilized to compute water surface elevations and depth-averaged current velocities for select historical hurricanes across an unstructured finite element mesh. The version of ADCIRC employed is two-dimensional, depth-integrated, and solves the continuity and momentum equations (Kolar et al., 1994; Luettich Jr. et al., 1992; Luettich and Westerink, 2004; Westerink et al., 2008). The 1.4 million node and 2.7 million element mesh is a modified version of the CPRA2017 mesh, which was developed for the Louisiana Coastal Protection and Restoration Authority of Louisiana (CPRA)'s 2017 Coastal Master Plan. The mesh spans the western north Atlantic Ocean (from the 60°W meridian), Caribbean Sea, and Gulf of Mexico and highly resolves the coastal features along the Gulf of Mexico from Mobile Bay, Alabama to the Bolivar Peninsula, Texas. It incorporates the most recent elevation data of south Louisiana and is an updated version of the CPRA2012 mesh (Cobell et al., 2013). Only wind and pressure forcings are included in this surge analysis. Waves, tides and riverine discharges are not included for reasons as follows. The Louisiana coast features a diurnal micro-tidal regime with a range of 0.32 m (National Oceanic and Atmospheric Administration, 2018). In addition, Mississippi River discharge during the three hurricanes to be simulated would have minimal influence on the results. Finally, to specifically examine the interaction of surge with the landscape, waves are not included. Future efforts can build in these complexities, but for the present study simplicity is warranted in this preliminary examination.

To study the change in coastal storm surge through time, the representation of the historic landscape in storm surge models must be comparable to the landscape presented in modern (2017) models. Since relatively few levees existed in south Louisiana in the mid-1800s, except Mississippi River levees (Barry, 2007; Campanella, 2008), and levees south and west of the Mississippi River have substantially changed since the mid-1800s, the levees in this area are removed from the high resolution storm surge model mesh of modern day coastal Louisiana. This allows for the proper evaluation of the temporal impact of wetland loss on storm surge across coastal Louisiana. This high resolution mesh with levees removed is utilized throughout this analysis and is referred to as the “detailed model”. This new name allows for the distinction of this model from the “simple model” which is created by applying the L:W isopleths to the detailed model.

4. Model simplification and basis of assessment

4.1. L:W isopleth description and derivation

In this analysis, a L:W isopleth is defined as a line that connects points of constant percent of land with respect to water along the Louisiana coast. L:W isopleths are derived for the year 2010 from satellite imagery and the ratio of land surface area to water surface area within a specified bounding box along the Louisiana coastal landscape (Gagliano et al., 1970, 1971; Twilley et al., 2016). L:W isopleths are employed to develop a simplified version of the detailed model of coastal Louisiana. Due to the diurnal micro-tidal regime along the Louisiana coast, a tidal range of 0.32 m, tides are not included in the derivation of L:W isopleths (National Oceanic and Atmospheric Administration, 2018).

The L:W ratio of the 2010 Louisiana coastal landscape is produced using spatial analysis of a land-water image derived from satellite imagery. A 101 m × 101 m neighborhood moving window operator is applied to the binary land-water raster image. An analytical function calculates the ratio of land-to-water inside the macro-sized floating window and assigns the result to the center pixel of the window. Each pixel in the region is independently analyzed. The result is a continuous pixel-by-pixel representation of the land-water ratio in the neighborhood of each pixel from which discrete intervals are vectorized as isopleth lines in a GIS framework. An isopleth representing any integer value of landwater ratio from 1 to 99 is possible. In addition, a color scale can be applied to the continuous image to simultaneously represent the full range of ratio values. The 2010 L:W isopleths include: 1%, 10%, 20%, 30%, 40%, 50%,

60%, 70%, 80%, 90%, 99% (Fig. 1a). For example, seaward of the 1% isopleth the area comprises entirely of water. At progressively larger distances inland from the 1% isopleth, the percentage of land increases until the 99% isopleth is reached indicating 99% land and 1% water. Areas further inland of this isopleth consist entirely of land.

4.2. Application of isopleths for surge model modification

The L:W isopleths are used to systematically simplify the Louisiana coastal landscape as represented in the detailed model and are used to identify general elevation polygons of “Submersed” (i.e. open water to wetland), “Intermediate” (i.e. wetland), and “High” (i.e. high wetland). Constant elevation and bottom roughness values (i.e. Manning's n) are assigned to each polygon. In this process of simplifying the detailed model the unstructured mesh topology is not altered (i.e. node count and location remains unchanged). Established major waterways, barrier islands and interior ridges also remain unchanged.

To simplify the detailed model via L:W isopleths, bands are first established between each of the eleven 2010 isopleths (Fig. 1b). These bands are then grouped together to form polygons for Submersed, Intermediate and High (for example: 99% > High > 90%; 90% > Intermediate > 40%; 40% > Submersed > 1% > Open water) (Fig. 1c). The Intermediate polygon is created, for instance, by selecting the bands between 40% and 90%. Elevations across selected bands within this polygon are averaged from all mesh nodes within the polygon from the detailed model and are assigned to all mesh nodes in the entire Intermediate polygon. This process is repeated for the Submersed and High polygons. Therefore, in each respective polygon (High, Intermediate, Submersed), all nodes have the same value for elevation. A Gaussian smoothing function is applied at each elevation transition: Open Water to Submersed, Submersed to Intermediate, and Intermediate to High. In the case of Manning's n , values are assigned to the three polygons in each model according to the dominate vegetation type in each polygon as described in literature: High: 0.070 (Estuarine scrub/scrub wetland), Intermediate: 0.045 (Brackish marsh), and Submersed: 0.025 (Open water) (Bilskie et al., 2015; Bunya et al., 2010). Interior lake bathymetric elevations in the study area are also averaged and this value is assigned to each lake along with a Manning's n value of 0.025.

4.3. Down selection of L:W isopleth permutations

The purpose of applying L:W isopleths is to create a simple model that closely reproduces the detailed model results. As introduced in the previous section, the L:W isopleths utilized were derived for the year 2010 and include: 1%, 10%, 20%, 30%, 40%, 50%, 60%, 70%, 80%, 90%, 99% (Fig. 1a). To establish polygons with the same elevation and Manning's n values discussed in the previous section, the possible number of L:W isopleth permutations is down selected (i.e. narrowed) to find the best possible isopleth permutation that creates the most accurate simple model with respect to the detailed model.

The study area is bounded by the Intracoastal Waterway (ICWW) or 99% isopleth (north) and 1% isopleth (south) as these isopleths represent nearly 100% land and nearly 100% water, respectively. In instances where the 99% isopleth extends north of the ICWW, the ICWW is chosen as the northern most boundary as this canal has been generally fixed in place since 1925 (Harrison, 2015). The number of possible isopleth permutations without repetition is therefore 9! or 362,880. Only two of these nine isopleths are used to create simple models resulting in a total 72 models that could be developed. However, half of these permutations, 99%–80%–90%–1% for example, are unrealistic due to the L:W isopleths not being in descending order. Therefore, a total 36 simple models are created.

4.4. Storm surge simulations

The detailed model and 36 simple models are forced with meteorological wind and pressure fields for Hurricanes Katrina (2005), Rita (2005), and Gustav (2008) which are generated from an assimilation of objectively analyzed,

observed and modeled winds and pressures (Cox et al., 1995; Powell et al., 1998). These storms are selected because they made landfall and impacted the east, west and central areas of coastal Louisiana, respectively (Fig. 2). Simulating hurricanes with three different landfall locations provides three different Louisiana coastal landscape perspectives when attempting to find the “best fit” isopleth permutation. Rita struck the Chenier Plan (CP) in southwest Louisiana, Gustav both the CP and MRD in south central Louisiana and Katrina the MRD in southeast Louisiana. The simulation output for each hurricane derived with the detailed model is compared to the output for each respective hurricane derived with all 36 simple models. This comparison of results reveals which simple model (i.e. which permutation of L:W isopleths) most closely resembles the detailed model.

4.5. Application of hydrologic unit code 12 in surge quantification

The 2014 U.S. Geological Survey (USGS) hydrologic unit code 12 (HUC12) sub-watershed basins are utilized to quantify simulated storm surge model output and to compare detailed model and simple model results (Seaber et al., 1975, 1987; United States Geological Survey, 2015). HUC12 sub-watersheds are uniquely employed to compare the storm surge model featuring a detailed model and the simple models results. These sub-watersheds provide geographical bounds for which maximum water surface elevations (max WSEs) and volume of inundation are quantified in the landfall region as well as remote areas. This metric defines how local features impact storm surge responses. The output of results (max WSEs and volume) from the detailed model and all 36 simple models within each HUC12 are compared on a HUC12 by HUC12 basis (detailed model vs. simple model) to calculate the mean absolute maximum water level difference (m) and mean percent error in volume inundated.

5. Results

5.1. Simple model description

A total 36 simple models are created using various permutations of the L:W isopleths. For each simple model, an average topographic elevation value is



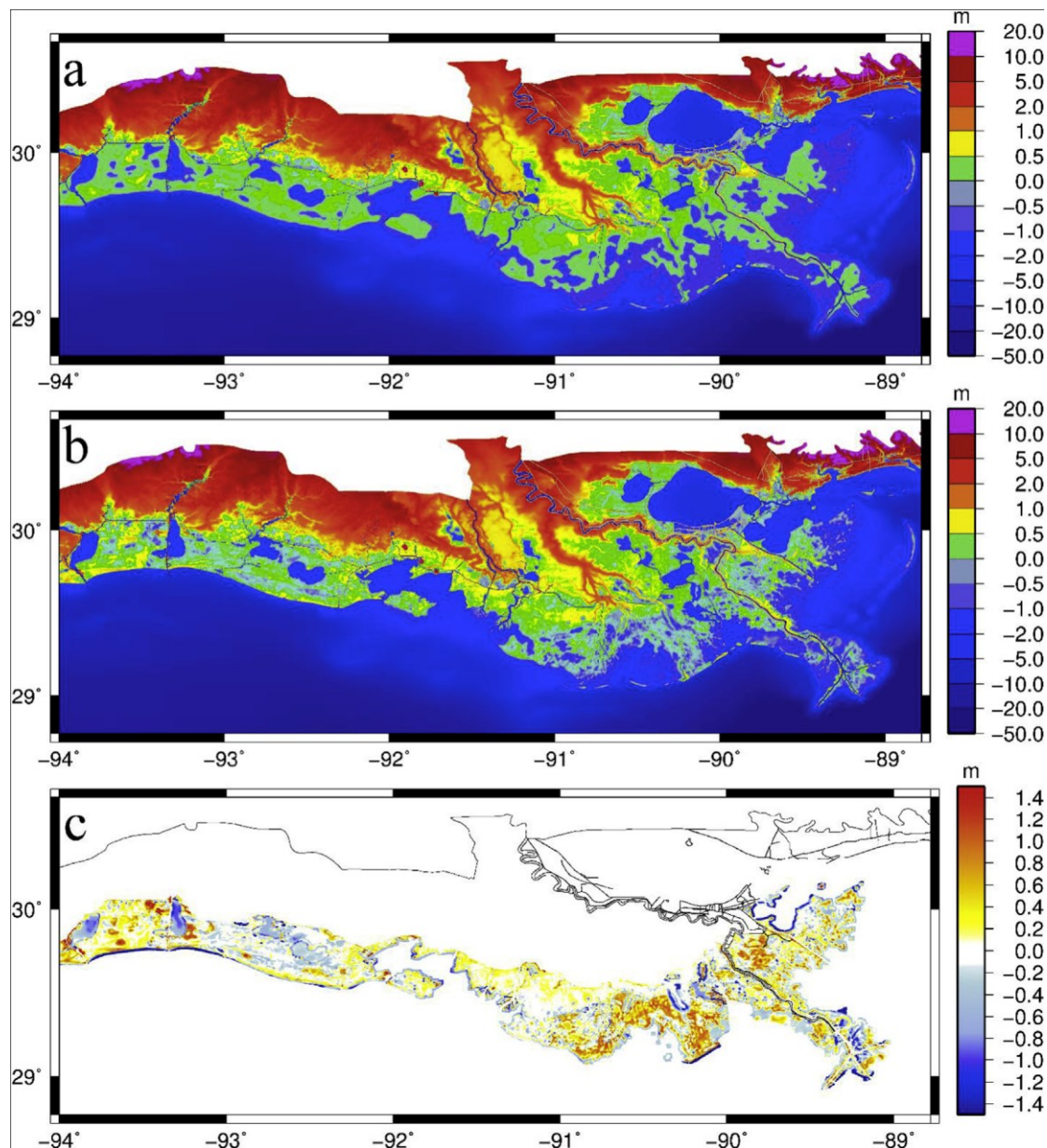
Fig. 2. Tracks of hurricanes simulated in this study: Katrina (black), Gustav (white) and Rita (dotted).

Fig. 3. a) Topo-bathymetric landscape of the simple model (99%–90%–40%–1%) with respect to NAVD88. b) Topo-bathymetric landscape of the detailed model with respect to NAVD88. c) Elevation difference plot: detailed model – simple model.

found and assigned to the polygons labeled High, Intermediate and Submersed. Manning's n bottom roughness values of 0.070, 0.045, and 0.025 are also assigned, respectively, to the three polygons, for all simple models. Hurricane Katrina, Rita and Gustav wind and pressure forcing are simulated with each of the 36 simple models and with the detailed model for a total of 111 storm surge simulations. Hydrologic unit code 12 (HUC12) sub-watersheds are employed to find the mean maximum water surface elevation and mean volume inundation per HUC12 for each model. HUC12 sub-watersheds are also utilized to find the mean absolute maximum water level difference and mean percent error in volume inundated between each simple model and respective detailed model per HUC12.

For the 99%–90%–40%–1% simple model, the average topographic elevation values for the three polygons (with respect to NAVD88) are 0.47 m, 0.27 m, and 0.98 m for High, Intermediate, and Submersed, respectively. The topo-bathymetric landscape of this simple model (Fig. 3a and Fig. 4a) and detailed model (Figs. 3b and 4b) are presented. In the simple model, the 40% isopleth is clearly indicated by the distinct interface between green (Intermediate) and gray (Submersed) elevation values along the Louisiana coast (Fig. 4a). Fragmented wetlands depicted in the detailed model convert to Intermediate and Submersed in the MRD for the simple model. The elevation difference between the simple and detailed models and the conversion of fragmented wetlands is indicated by the warm colors in the MRD (Fig. 3c). The difference in elevation ranges generally from 1 m to 1 m NAVD88. Manning's n bottom roughness values for this simple model are presented in Fig. 5a. Manning's n values for the detailed model are shown in Fig. 5b. Areas north of the ICWW remain unchanged in both models. The simple model also generally simplifies the fragmented wetland vegetation.

Topo-bathymetric cross-sectional profiles are obtained within the Atchafalaya (A–A⁰) and Terrebonne (B–B⁰) regions for the simple and detailed models to contrast the sediment abundant (Atchafalaya) and



sediment starved (Terrebonne) landscapes (Fig. 4). Profiles A^-A^0 and B^-B^0 are taken in the same location for each model. Profile A^-A^0 begins near the ICWW (A) and ends in the Atchafalaya Bay (A^0) (Fig. 4c) and profile B^-B^0 (Fig. 4d) begins on a ridge and ends in the Gulf of Mexico near Raccoon Island. For profile A^-A^0 , the cross-section of the simple model (orange line) closely follows that of the detailed model (gray line) with an average absolute difference of 0.11 m between both cross sections, which is approximately 4.6% of the elevation range and a variance of 0.02 m^2 . The general trend of land elevations are similar and the location of the shoreline where elevations rapidly reduce is captured in the simple model. Wetland fragmentation is minimal across A^-A^0 whereas substantial wetland fragmentation occurs across B^-B^0 . Nonetheless, the simple model (orange line) follows the general trends of the detailed model (gray line) and contains an average absolute difference of 0.21 m, which is approximately 9.3% of the elevation range and a variance of 0.07 m^2 . The increase in wetland fragmentation is reflected by a greater variance in B^-B^0 where the landscape contains larger fluctuations in elevation across the profile. For example, from approximately 6–20 km along profile B^-B^0 , the

simple model reflects the average elevation of the detailed model well. In addition, large water bodies are also reflected in the simple model, such as from 2 to 6 km and 20–28 km in B^-B^0 .

Maximum water surface elevations are presented for Hurricanes Rita (Fig. 6a and b), Gustav (Fig. 6c and d) and Katrina (Fig. 6e and f) for the 99%–90%–40%–1% simple model (Fig. 6a, c and e) and the detailed model (Fig. 6b, d and f) for the duration of each simulation. Maximum peak surge occurs in southwest Louisiana east of the storm track during Rita and is approximately 4.5 m (NAVD88). A 3 m surge is simulated east of the Mississippi River due to the local geometry of the Mississippi River levees (Fig. 6a and b). Peak surge for Gustav is approximately 3.5 m (NAVD88) and occurs east of the Mississippi River due to the geometry of the Mississippi River levees, steep elevation gradients along the Mississippi Gulf Coast and the broad and shallow continental shelf between these two raised topographic features (Fig. 6c and d). In a similar fashion for Katrina, a peak surge greater than 8.0 m occurs along the Mississippi coast.

The mean maximum water surface elevation is computed for Rita

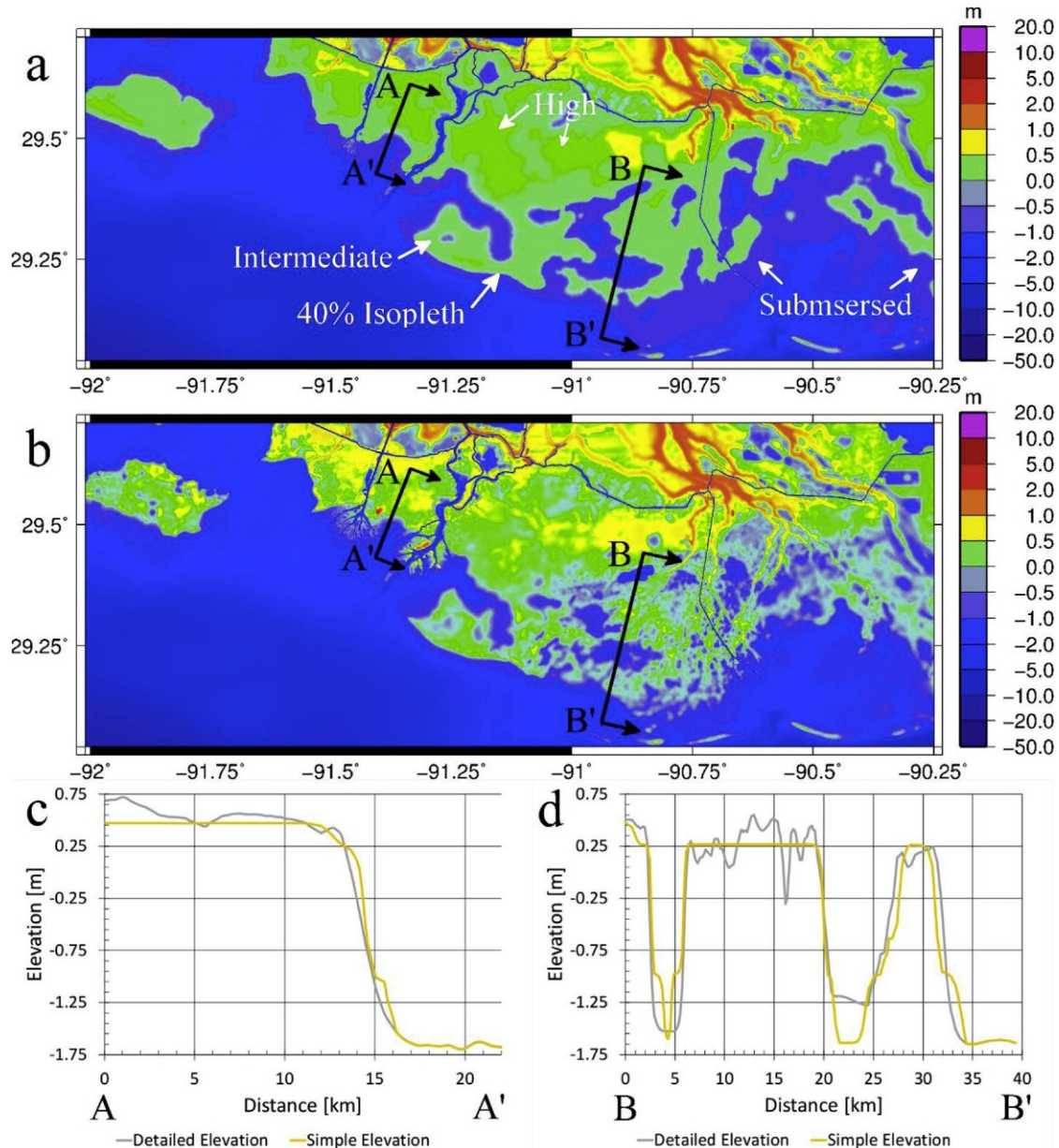


Fig. 4. a) Location of profiles A^-A^0 and B^-B^0 in the simple model (99%–90%–40%–1%). b) Location of profiles A^-A^0 and B^-B^0 in the detailed model. c) Topobathymetric (m, NAVD88) cross-section of the simple model (orange) and detailed model (gray) at A^-A^0 . d) Topo-bathymetric (m, NAVD88) cross-section of the simple model (orange) and detailed model (gray) at B^-B^0 . (For interpretation of the references to color in this figure legend, the reader is referred to the Web version of this article.)

(Fig. 7a and b), Gustav (Fig. 7d and e) and Katrina (Fig. 7g and h) per each HUC12 for the 99%–90%–40%–1% simple model (Fig. 7a, d and g), the detailed model (Fig. 7b, e and h) along with the mean absolute maximum water level difference (simple – detailed model results) for each storm (Fig. 7c, f and i). For Rita, this difference ranges from 0.19 m to 0.23 m with four of the total 373 HUC12s in the range of 0.15 m–0.23 m (red), six HUC12s between 0.10 m and 0.15 m (red-orange), eight in the range of 0.19 m to 0.15 m (dark green) and 19 between 0.15 m and 0.10 m (green). Therefore, 336 of the 373 HUC12 values are between 0.10 m (light green, white and orange) and 252 of the 373 in the

range of 0.05 m (white) (Fig. 7c). Similarly, for Gustav, the difference ranges from 0.21 m to 0.23 m with 331 of the total 366 HUC12s values in the range of 0.10 m (light green, white, orange) and 246 of the total 366 HUC12 values between 0.05 m (white) (Fig. 7f). Regarding Katrina, the difference ranges from 0.24 m to 0.21 m with 323 of the total 363 HUC12 values in the range of 0.10 m (light green, white, orange) and 272 of the total 363 HUC12 values in the range of 0.05 m (white) (Fig. 7i). Generally, the simple model surge results are higher along the coast and lower inland relative to the detailed model for all three storms (Fig. 7c, f and i), particularly on the east side of each storm. However, cross sections where the greatest WSE differences occur (Fig. 8 and Fig. 9) reveal the simple model overall accurately reproduces the WSEs of the detailed model.

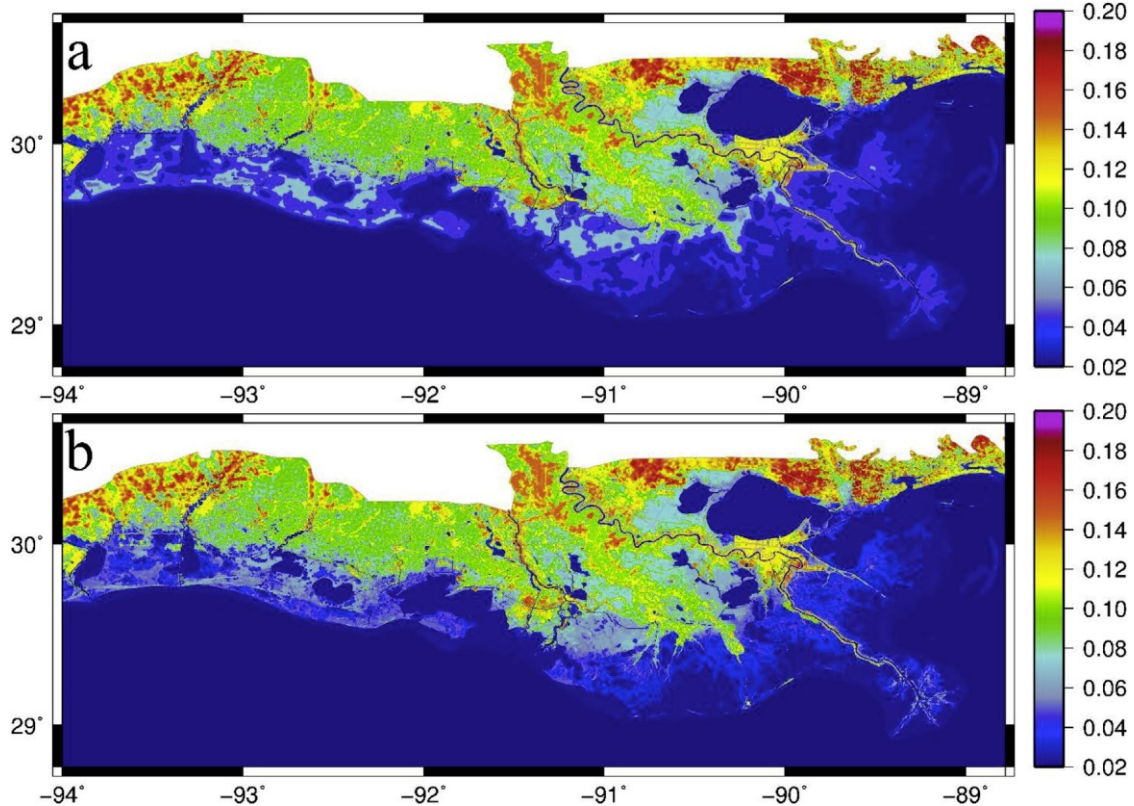


Fig. 5. a) Manning's n values of the simple model (99%–90%–40%–1%). b) Manning's n values of the detailed model.

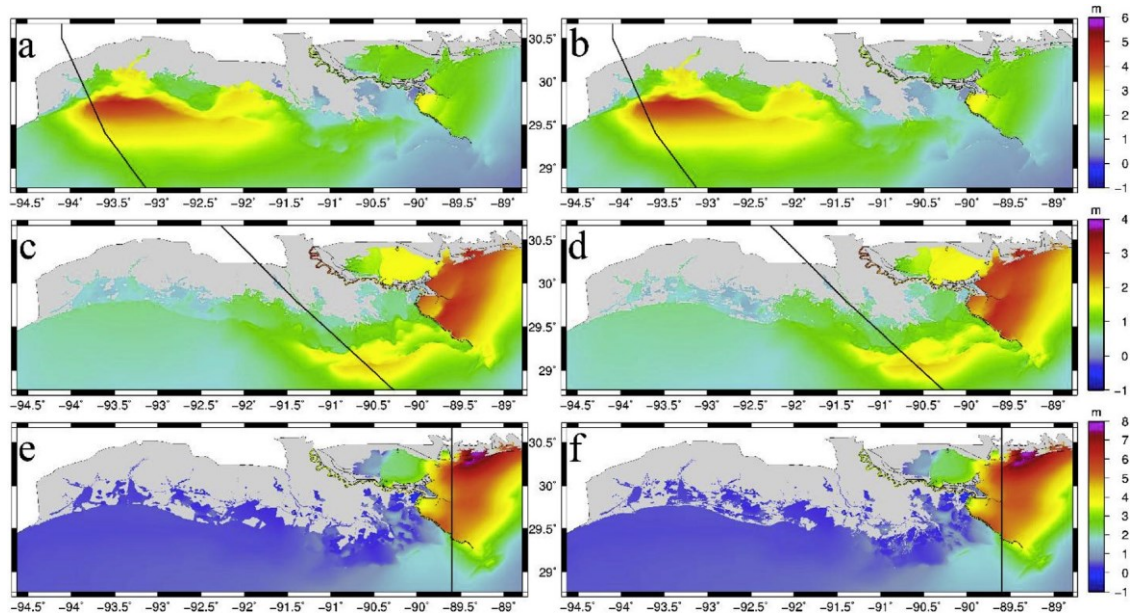


Fig. 6. Maximum water surface elevations (m, NAVD88) for: Rita simple model (99%–90%–40%–1%) (a) and detailed model (b), Gustav simple model (c) and

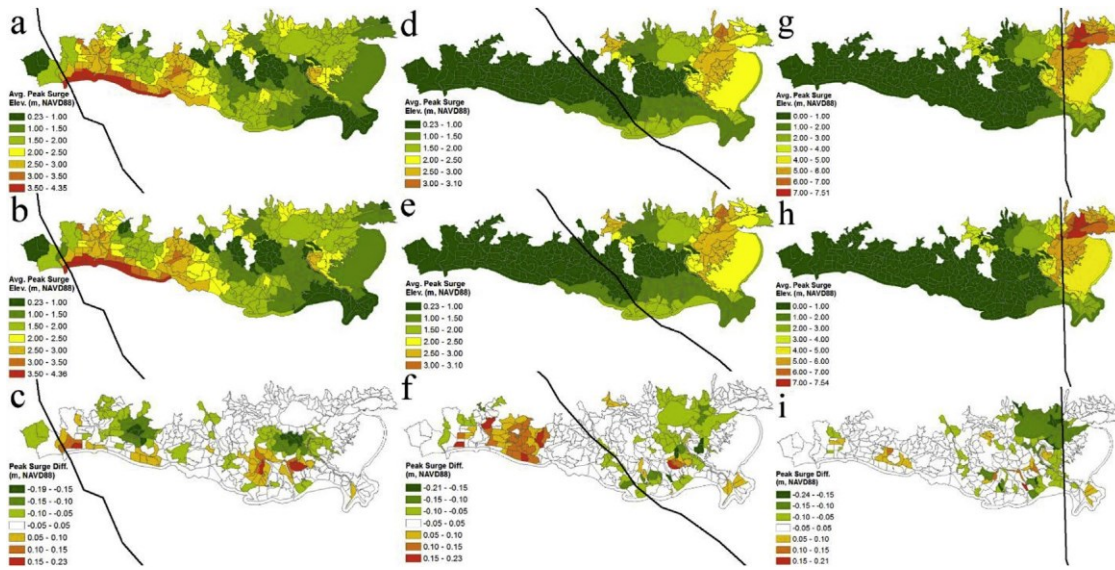
To investigate the WSE differences further, two cross-sectional profiles are taken from the Hurricane Rita (Fig. 8) and Gustav (Fig. 9) results: one across the Chenier Plain (CP) in southwest Louisiana and another across the Mississippi River Delta (MRD) in southeast Louisiana. Overall these profile plots demonstrate that the WSE results from the simple model generally mirror those of the detailed model. For instance, profile A-A⁰ of Fig. 8b reveals two topobathymetric elevation values of the simple model (orange) between approximately 32 km and 54 km which accurately resemble the irregular topobathymetric elevation profile

detailed model (red), the WSE of the simple model (red)

accurately reproduces the WSE produced by the detailed model (blue). Profile

B-B⁰ reveals an overall similar trend but with WSE differences between 32 km

and 60 km. In this area, the simple model topobathymetric elevation is higher



and the WSE elevation is also higher relative to that of the detailed model (Fig. 8c). For both profiles, the reverse occurs north of the ICWW with the topo-bathymetric elevations remaining the same for both models while the WSE for the simple model is lower than that of the detailed model. In addition, profile B

B^0 of Fig. 9c reveals WSE differences for Gustav between the simple (red) and detailed (blue) models to be negligible whereas Fig. 9b reveals relatively greater differences between the WSEs of the detailed and simple models

Fig. 7. Mean maximum water surface elevations for Rita (a,b,c), Gustav (d,e,f), Katrina (g,h,i), with respect to NAVD88 per hydrologic unit code 12 (HUC12) subwatersheds for the simple model (99%–90%–40%–1%) (a,d,g), detailed model (b,e,h), and mean absolute maximum water level difference (simple model – detailed model) (c,f,i).

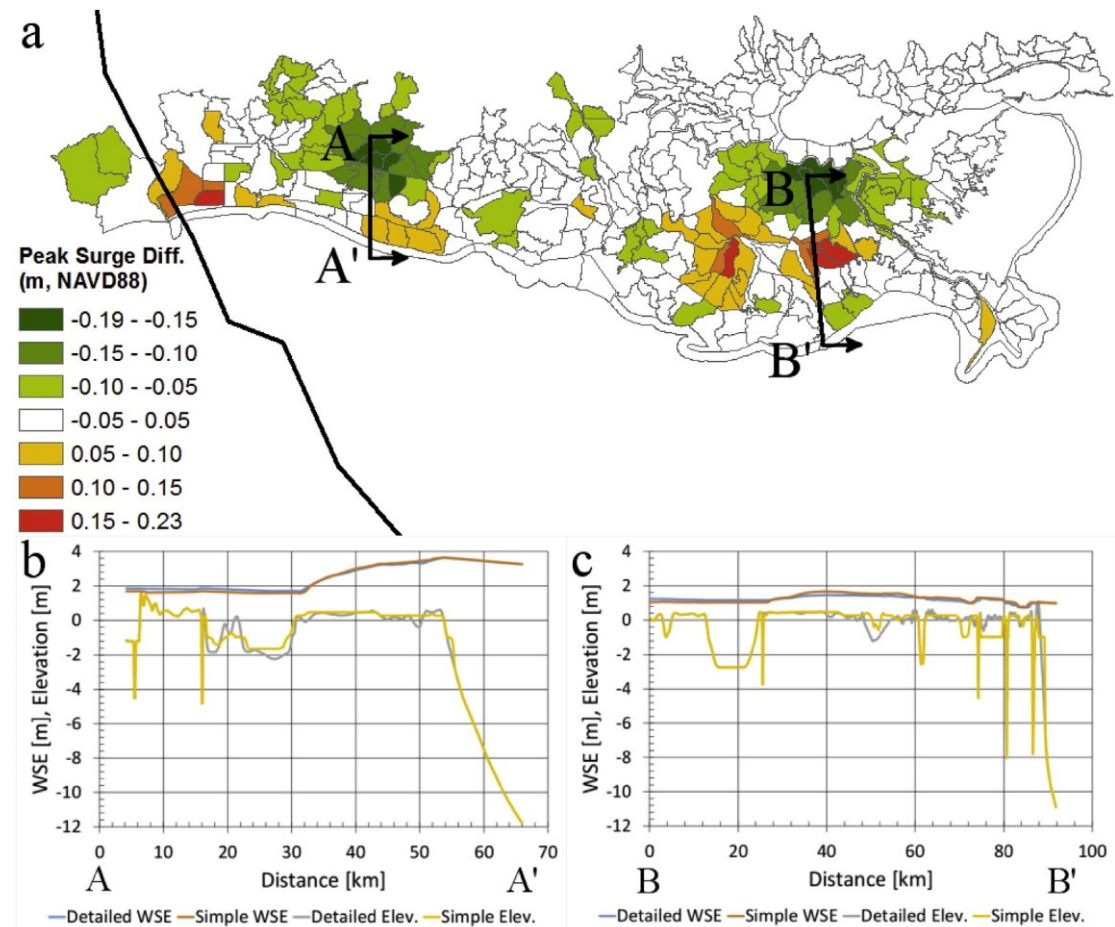


Fig. 8. a) Location of profiles A–A' and B–B' in relation to mean absolute maximum water level difference (simple model – detailed model) for Rita. b) Cross-section of the water surface elevation (WSE) for detailed (blue) and simple (red) models and topo-bathymetric (m, NAVD88) cross-section of the detailed (gray) and simple (orange) models at A–A'. c) Cross-section

of the water surface elevation (WSE) for detailed (blue) and simple (red) models and topo-bathymetric (m, NAVD88) crosssection of the detailed (gray) and simple (orange) models at B^-B^0 . (For interpretation of the references to color in this figure legend, the reader is referred to the Web version of this article.)

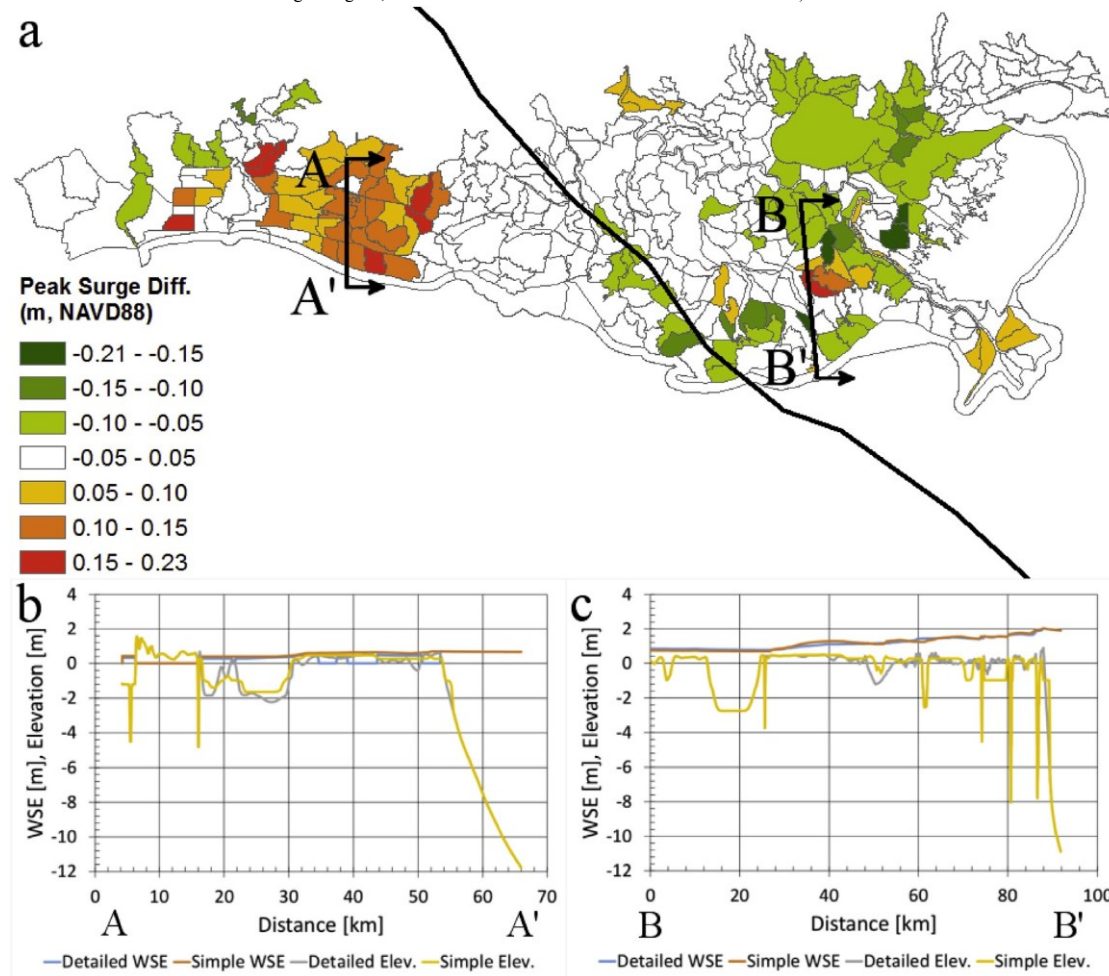


Fig. 9. a) Location of profiles A^-A^0 and B^-B^0 in relation to mean absolute maximum water level difference (simple model – detailed model) for Gustav. b) Cross-section of the water surface elevation (WSE) for detailed (blue) and simple (red) models and topo-bathymetric (m, NAVD88) crosssection of the detailed (gray) and simple (orange) models at A^-A^0 . c) Cross-section of the water surface elevation (WSE) for detailed (blue) and simple (red) models and topo-bathymetric (m, NAVD88) crosssection of the detailed (gray) and simple (orange) models at B^-B^0 . (For interpretation of the references to color in this figure legend, the reader is referred to the Web version of this article.)

indicating the importance of small topographic differences during low WSE events.

5.2. Surge results for all 36 simple models

The isopleth permutations are listed in the same order (Fig. 10, Fig. 11) and this order is based on the mean absolute maximum water level difference per HUC12 with respect to NAVD88 (Fig. 10). For the mean absolute maximum water level difference quantification, the simple model with the lowest error is 99%–90%–40%–1%. This model yields a mean absolute maximum water surface elevation difference of 0.042 m for Hurricane Rita when compared to the results of the detailed model. For Hurricanes Gustav and Katrina, the simple model that most closely resembles the detailed model is 99%–80%–40%–1% with mean absolute difference values of 0.043 m and 0.034 m, respectively. However, the 99%–90%–40%–1% simple model results reveal a negligible difference between these two models with mean absolute difference values of

0.044 m (Gustav) and 0.035 m (Katrina). For Hurricane Rita, the 99%–80%–40%–1% simple model ranks seventh with a mean absolute difference of 0.056 m. The simple model with the greatest error is 99%–20%–10%–1% with differences of 0.214 m (Rita), 0.115 m (Gustav) and 0.105 m (Katrina).

A small number of hydrologic basins yield substantial errors for the mean percent error in volume inundated computation. Therefore, for each simple model to detailed model comparison, the top 5 percent of HUC12s with the greatest error is removed and only the lowest 95 percent of HUC12s is considered. The simple model with the lowest error is also 99%–90%–40%–1% when all three storms are considered with errors of 3.4%, 11.4% and 10.2% for Rita, Gustav and Katrina, respectively (Fig. 11). For Rita, errors range from 3.2% to 16.5% for the 99%–90%–50%–1% and 99%–20%–10%–1% simple models. For Gustav, errors range from 10.7% to 18.7% for the 99%–80%–40%–1% and 99%–30%–10%–1% simple models. Lastly, the percent error volume

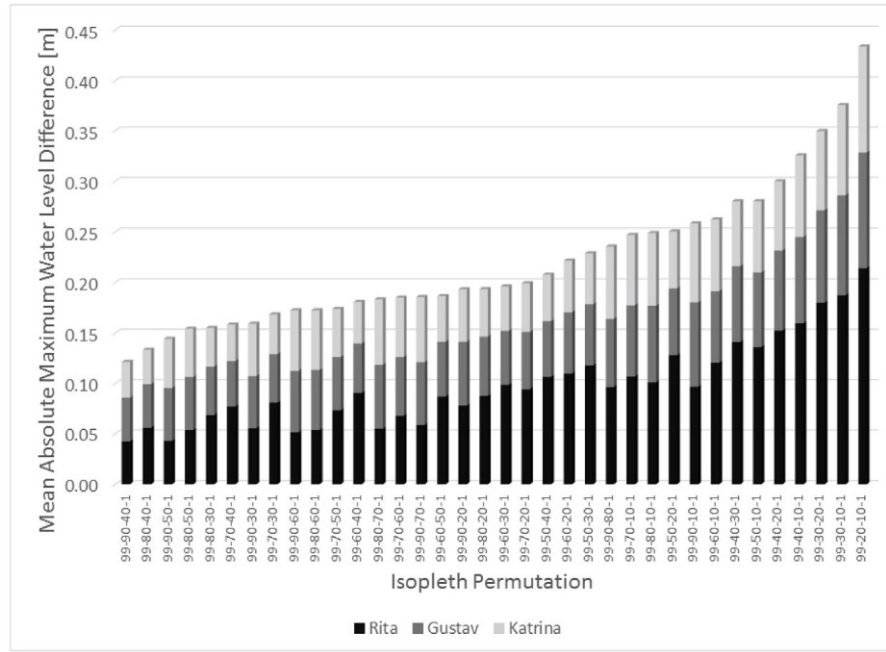


Fig. 10. Mean absolute maximum water level difference (m) of all HUC12 sub-watersheds for Hurricanes Rita, Gustav, Katrina for each of the 36 simple models vs the detailed model.

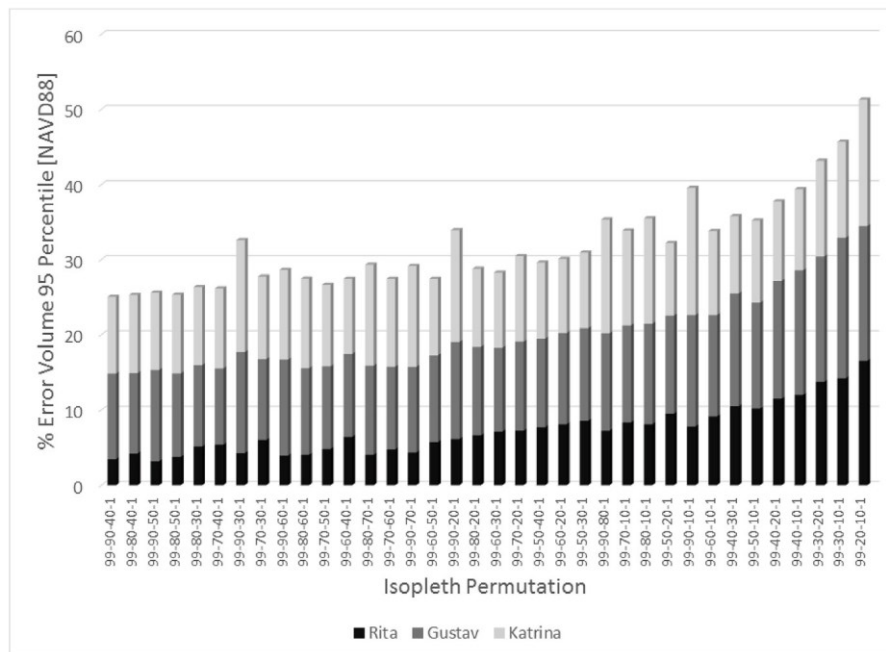


Fig. 11. Mean percent error in 95 percentile volume inundated of all HUC12 sub-watersheds for Hurricanes Rita, Gustav, Katrina for each of the 36 simple models vs ranges from 10.2% to 16.9% for the 99%–90%–40%–1% and 99%–20%–10%–1% simple models for Katrina.

6. Discussion

6.1. Establishment of L:W isopleth approach

The mean absolute maximum water level difference and mean percent error volume inundated are used to identify the L:W isopleth permutation that yields a simple model which closely resembles the detailed model in both landscape features and storm surge response. Therefore, the 99%–90%–40%–1% isopleth

permutation is identified as the "best-fit" simple model and is henceforth referred to only as "simple model". The mean absolute difference of the maximum water surface elevation between the detailed model and simple model for Rita is the detailed model.

0.042 m with maximum values not exceeding 0.23 m or 0.19 m (Fig. 7c). For Gustav, the mean difference is 0.044 m with a range of 0.21 m to 0.23 m (Fig. 7f) and for Katrina the mean difference is 0.035 m with a range of 0.24 m to 0.21 m (Fig. 7i). The mean percent error in volume inundated per HUC12 for all three storms also supports the simple model as the closest representation of

the detailed model by having collectively the lowest error of all 36 simple models (Fig. 11).

Simplifying the modern Louisiana coastal landscape using L:W isopleths has many benefits. Because the isopleths are obtained solely from satellite imagery, they are derived irrespective of the geologic, sea level, wetlands or human migration processes ongoing at the time the satellite imagery is taken. Therefore, the same methodology could be applied to both the retrograding Mississippi River Delta (MRD) and the prograding Chenier Plain (CP). In addition, this methodology effectively accounts for wetland fragmentation along the Louisiana coast and emphasizes the importance of a solid, unfragmented land mass in the reduction of storm surge along the Louisiana coast. Fragmented wetlands in the MRD depicted in the detailed model convert to Intermediate and Submersed in the simple model (Fig. 4). The fragmented wetlands that convert to Intermediate and Submersed also corresponds with the areas of substantial land loss along the Louisiana coast (Blum and Roberts, 2012). This can also be seen in the cross-sectional profiles A⁻A⁰ and B⁻B⁰ (Fig. 4). The simple model cross-sectional profile closely follows that of the detailed model (Fig. 4c) in the sediment abundant Atchafalaya Delta area while the simple model profile does not follow that of the detailed model (Fig. 4d) as closely in the sediment starved Terrebonne Bay area.

Additional benefits of employing L:W isopleths include the ability to create comparable storm surge models for different time eras. A surge model developed using, for instance, 1930s data (bathymetry, topography, and land cover), could not be compared to a surge model developed in 2010 using “state of the art” technology to collect bathymetric, topographic, and land cover data from that era. This is due to the relatively primitive data collection methods of the 1930s and resulting substantial absence of topo-bathymetric data across the Louisiana coast for this time period. However, L:W isopleths have the capability to link these two eras through use of the similar methodologies to derive the isopleths for both eras and, for example, through the application of the elevation and Manning's n values utilized in each 2010 coastal zone to each respective coastal zone in 1930 with the extent of the 1930 coastal zones determined by the 1930 L:W isopleths. Similarly, comparable surge models could also be constructed for other eras such as 1970 and 2000 to gain even more insight into changes in storm surge along coastal Louisiana through time.

Establishing the 99%–90%–40%–1% simple model as the most accurate simplified representation of the modern Louisiana coast is significant because Twilley et al. (2016) showed the far inland migration of the 50% isopleth between the years 1930 and 2010 especially in Terrebonne Parish. The 50% isopleth is located near the 40% isopleth for 2010. Because the 50% L:W isopleth is much closer to the Gulf of Mexico in 1930 compared to 2010 in Terrebonne Parish (Twilley et al., 2016), there are likely substantial differences in surge response in this area for these two time periods due to the changes in the coastal landscape in this area.

Yet another benefit of applying L:W isopleths to simplify the detailed model is the potential increase in computational efficiency and decrease in simulation wall clock time through coarsening the simple model mesh. The simple model mesh was not coarsened in this study. However, for a mesh with a high-density node count, this methodology could be adapted to increase horizontal mesh resolution and thereby reduce the mesh node count increasing computational efficiency.

6.2. Broader findings and implications

The U.S. Army Corps of Engineers (1963) established that storm surge is reduced one vertical meter for every 14.5 horizontal kilometers of coastal wetlands. However, this analysis and more recent analyses (Lawler et al., 2016; Loder et al., 2009; Resio and Westerink, 2008; Wamsley et al., 2010) show this is an over simplification of the surge-wetland relationship and numerical models that accurately simulate coastal processes should be employed. This is confirmed with the profiles shown in Figs. 8 and 9. In profile A⁻A⁰ of Fig. 8,

surge attenuates exponentially from approximately 3.8 m⁻² m over about 22 km of mostly continuous wetlands (or approximately 1 m per 13.75 horizontal km) for both the simple and detailed models. In profile B⁻B⁰, surge reaches a height of approximately 1.8 m about 47 km inland for the simple model (about 1.6 m detailed model) and does not decrease to 1.0 m for both models until about 60 km inland. Therefore, in profile B⁻B⁰, surge builds from the coast until approximately 47 km inland and is not substantially reduced until approximately 60 km inland even though there are 47 km of fragmented wetlands between the Gulf of Mexico and the location of maximum surge height. In profile A⁻A⁰ of Fig. 9, the low surge generated on the west side of Gustav is attenuated by a coastal Chenier ridge for the detailed model and propagates further inland for the simple model due to the lowering of this ridge in the simplifying process. In profile B⁻B⁰, surge reduces linearly from 2 m to approximately 0.8 m over 60 km (or approximately 1 m per 50 horizontal km).

In addition, Resio and Westerink (2008) found that for a fast moving storm like Hurricane Rita the maximum inland attenuation rates range from 1 m per 11 km to 1 m per 19 km in southwest Louisiana. Resio and Westerink (2008) also found in southeast Louisiana, where winds were constant in direction and magnitude for a long period of time, surge increases up to the Mississippi River levee near English Turn 40 km inland from the Gulf of Mexico. This shows that wetlands provide frictional resistance to surge for only a limited period. These findings along with those shown in Figs. 8 and 9 confirm surge attenuation cannot be described by a single rule of thumb because this simple rule does not consider details such as storm forward speed and the diminished surge reduction capability of wetlands associated with stationary storms. Therefore, storm surge attenuation is governed by many factors including but not limited to storm size, wind velocity, duration, landfall location and regional topo-bathymetry.

Wetland fragmentation also influences surge attenuation rates. As indicated by this study and other studies (Gagliano et al., 1970, 1971; Twilley et al., 2016), L:W isopleths capture the decay of the MRD on a broader scale while highlighting the resilience of the Wax Lake and Atchafalaya Deltas (Bentley et al., 2016; Blum and Roberts, 2012; Roberts, 1997). These two deltas reveal the importance of a solid, unfragmented land mass in the reduction of surge. When converted to only land or only water (i.e. no fragmented wetlands along the coast) the Louisiana coastline moves farther inland in the MRD, east of the Wax Lake and Atchafalaya deltas, but remains in approximately the same location along these deltas and along the CP west of the Wax Lake and Atchafalaya Deltas (Fig. 3). This corresponds with findings of previous studies. Barbier et al. (2013) emphasizes the importance of unfragmented wetlands by showing a 1% increase in the wetland:water ratio reduces surge by 8.4%–11.2% along a transect in the Caernarvon Basin. Other studies have also shown storm surge reduction capabilities of fragmented wetlands decrease as surge depth increases (Lawler et al., 2016; Loder et al., 2009; Wamsley et al., 2010).

In addition, in profile B⁻B⁰ of Fig. 8, the water surface elevation (WSE) for the simple model is 1.8 m while that of the detailed model is about 1.6 m. As can be seen in Fig. 8c, the higher WSE for the simple model corresponds with a higher topo-bathymetric elevation than that of the detailed model. The same can be seen in profile B⁻B⁰ between 30 and 48 km (Fig. 9c). Conversely, north of the ICWW, the WSE in this region is lower for the simple model than the detailed model. However, topographic elevations are equal north of the ICWW for both models. Therefore, it is found that surge heights are reduced in lower wetland elevations and surge is able to penetrate further inland, whereas higher wetland elevations restrict inland flooding. This same phenomena was found by Loder et al. (2009) who tested an idealized wetland area featuring a constant size and roughness with varying topo-bathymetric elevations and surge heights. For a wetland elevation of 2.0 m and a surge height of 1.8 m, Loder et al. (2009) discovered surge heights are higher along the coast and lower farther inland relative to the same area with a wetland elevation of 0.5 m and surge height of 1.8 m.

Major local topo-bathymetric features can also substantially impact surge response. Three major local topo-bathymetric features: the Mississippi River levees, the ancient deltaic lobe of the Mississippi River and the Mississippi Gulf Coast influence surge heights across coastal Louisiana and coastal Mississippi (Fig. 6). For Katrina, surge elevations are raised between the Mississippi River levees and the state of Mississippi coast due to these three topo-bathymetric features (Chen et al., 2008) and the northerly track of the storm across southeastern Louisiana. The counter-clockwise rotation of the hurricane causes surge to build between the levees and Mississippi coast and the shallow shelf elevates the surge (Fig. 6e and f). These factors result in high inland coastal flooding in Mississippi and along the northeast shoreline of Lake Pontchartrain. These high surge levels are also shown by Bunya et al. (2010) across coastal Louisiana and Bilskie et al. (2014) in the northern Gulf of Mexico. For Gustav, the maximum surge height does not occur at the location of landfall near Cocodrie, LA but between the Mississippi River levees and coastal Mississippi (Fig. 6c and d). For Rita, the maximum surge elevation occurs in southwest Louisiana near the landfall location; however, surge also builds between the Mississippi River levees and coastal Mississippi. For all three storms, the Mississippi River levees protect communities such as Houma and the Bayou Lafourche communities located on the west side of these levees and elevate surge in communities located on east side.

Minor local topo-bathymetric features are also important for reducing low storm surges. Relatively high mean absolute maximum water level differences occur in southwest Louisiana during Gustav on the west side of the storm track (Fig. 7f). Two profiles of topo-bathymetric and maximum water surface elevations (WSEs) are depicted in Fig. 9 for the simple and detailed models for Gustav, one in southwest Louisiana on the west side of the storm track (A^-A^0) and the other on the east (B^-B^0). There are substantial differences in the simple and detailed model maximum WSEs for profile A^-A^0 . This is due to the raised Chenier ridge located near the Gulf of Mexico between 50 and 54 km which prevents the low surge from propagating inland for the detailed model. However, this ridge is lowered in the simple model due to the assigning of the same elevation to all nodes in the Intermediate polygon. Therefore, land elevation is not as high between 50 and 54 km in the simple model allowing the low surge to propagate further inland resulting in large discrepancies between models for low surge. However, for high storm surge along the same transect (Fig. 8b) there is little discrepancy between the WSE for the simple and detailed models revealing small elevation differences in local topographic features become less important as surge height increases.

The Mississippi River Delta and the Chenier Plain are low-lying river dominated coastal areas created during the Holocene geologic period. The methodology to simplify the coastal landscape via L:W isopleths is applied with the goal of finding the isopleth permutation that best reproduces the surge output of the detailed model. This isopleth permutation can then be applied to historical eras to create comparable storm surge models and thus examine the change in coastal storm surge through time. While the 99%-90%-40%-1% isopleth permutation is determined the permutation that yields a simple model closest to that of the detailed model in coastal Louisiana, this same methodology can be applied to other similar coastal landscapes to find which permutation best corresponds with that location and to then examine the historical change in coastal hazards in that area. This methodology is most suitable for low-lying areas with substantial wetland fragmentation.

7. Conclusions

Results of this analysis show a simple storm surge model of the Louisiana coastal landscape can be developed to well-represent the surge characteristics of a detailed model of the Louisiana coast through the application of land to water (L:W) isopleths. HUC12 sub-watersheds are shown to be a useful instrument for result comparisons and surge assessments. A methodology is established to derive the L:W isopleths for the year 2010 and effectively apply the L:W isopleths to a detailed model of the Louisiana coast. The purpose of

establishing this methodology is to develop a simple model that closely reproduces the detailed model surge output.

It is discovered that the isopleth permutation of 99%-90%-40%-1% creates a simple model that yields surge results most similar to those of the detailed model. For Rita, Gustav and Katrina, the mean absolute difference in maximum water surface elevations between the two models is 0.042 m, 0.044 m and 0.034 m, respectively. For all three storms collectively, this is the smallest maximum water level difference compared to the detailed model. The 95 percentile of the mean percent error in volume inundated of all HUC12 sub-watersheds also reveals the 99%-90%-40%-1% simple model to collectively be the closest to the detailed model with errors of 3.4%, 11.4%, and 10.2% for Rita, Gustav and Katrina, respectively.

Results of this analysis support the view of Resio and Westerink (2008) and Wamsley et al. (2010) who claim numerical models that accurately simulate hydrodynamic processes, especially storm surge, should be employed to analyze storm surge attenuation in place of simple rules of thumb regarding surge attenuation. Rita simulation results reveal a nonlinear surge attenuation of approximately 1 m per 13.75 km of wetlands in southwest Louisiana and surge builds to 1.8 m approximately 47 km inland before reducing to 1 m approximately 60 km inland in southeast Louisiana. Gustav surge results also reveal varying surge attenuation rates in southwest and southeast Louisiana. Therefore, a constant attenuation rate per width of wetlands should not be utilized in the analysis of surge reduction. Numerical models with the ability to accurately simulate hydrodynamic processes should instead be employed.

Local topo-bathymetric features such as levees, coastlines and submerged shallow ancient deltaic lobes significantly influence surge heights and attenuation rates. The highest storm surge on record (9 m) was observed in Bay St. Louis, Mississippi during Hurricane Katrina in 2005. This surge height is successfully simulated in this analysis. Chen et al. (2008) also reproduced this surge height and showed that if the continental shelf had a greater depth and slope, the surge in this area would have only been 5 m. Chen et al. (2008) conclude the existence of the former deltaic lobe played a significant role in the record surge height and this is also confirmed through simulations performed in this analysis for Katrina, Gustav and Rita.

Results of previous work by Loder et al. (2009) are also confirmed through this analysis. Higher elevation and continuous (i.e. solid, unfragmented) wetlands along the coast results in relatively higher surge along the coast and relatively lower inland surge. The converse is also confirmed. Lower elevation and fragmented wetlands leads to lower surge heights along the coast and higher inland surge. Therefore, as more fragmented wetlands convert to open water thereby creating submerged shallow deltaic lobes, areas along the Louisiana coast that once attenuated surge will likely amplify it in the future. This will increase flood risk to currently upland communities across coastal Louisiana.

Finally, the methodology established can be applied in surge model development for various historical eras for the purpose of quantifying changes in Louisiana coastal storm surge through time. L:W isopleths represent a “snapshot” in time of the position of land and water along the Louisiana coast and are derived irrespective of the geologic, sea level, wetlands or human migration processes ongoing at the historical time in which they are derived. Therefore, the L:W isopleths serve as an important connector of historical eras to effectively study change in coastal storm surge through time. Next, historical storm surge models will be developed for this analysis of temporal change in coastal inundation, and therefore coastal flood risk.

Conflicts of interest None.

Acknowledgements

This work was supported by the Coastal SEES program of the National Science Foundation (NSF), [EAR-1533979 and EAR-1427389] and in part under the Louisiana Sea Grant Laborde Chair and the Louisiana Geological Survey. This work also used High Performance Computing at Louisiana State University (LSU) and the Louisiana Optical Network Initiative (LONI). The

statements and conclusions are those of the authors and do not necessarily reflect the views of NSF, Louisiana Sea Grant, LSU, or LONI.

This publication also made use of data sets provided by the Coastal Protection and Restoration Authority (CPRA) which were originally produced to inform the development of the 2017 Coastal Master Plan.

Appendix A. Supplementary data

Supplementary data related to this article can be found at <https://doi.org/10.1016/j.coastaleng.2018.03.006>.

References

- Ali, A., 1999. Climate change impacts and adaptation assessment in Bangladesh. *Clim. Res.* 12 (2–3), 109–116.
- Atkinson, J., McKee Smith, J., Bender, C., 2012. Sea-level rise effects on storm surge and nearshore waves on the Texas coast: influence of landscape and storm characteristics. *J. Waterw. Port. Coast. Ocean Eng.* 139 (2), 98–117.
- Babier, E.B., Georgiou, I.Y., Enchelmeyer, B., Reed, D.J., 2013. The value of wetlands in protecting southeast Louisiana from hurricane storm surges. *PLoS One* 8 (3) e58715.
- Barry, J.M., 2007. Rising Tide: the Great Mississippi Flood of 1927 and How it Changed America. Simon and Schuster.
- Bentley, S.J., Blum, M.D., Maloney, J., Pond, L., Paulsell, R., 2016. The Mississippi river source-to-sink system: perspectives on tectonic, climatic, and anthropogenic influences, miocene to anthropocene. *Earth Sci. Rev.* 153, 139–174.
- Bilskie, M.V., Coggins, D., Hagen, S.C., Medeiros, S.C., 2015. Terrain-driven unstructured mesh development through semi-automatic vertical feature extraction. *Adv. Water Resour.* 86, 102–118.
- Bilskie, M.V., Hagen, S.C., 2013. Topographic accuracy assessment of bare earth lidar-derived unstructured meshes. *Adv. Water Resour.* 52, 165–177.
- Bilskie, M.V., et al., 2016a. Dynamic simulation and numerical analysis of hurricane storm surge under sea level rise with geomorphologic changes along the northern Gulf of Mexico. *Earth's Future* 4 (5), 177–193.
- Bilskie, M.V., et al., 2016b. Data and numerical analysis of astronomic tides, wind-waves, and hurricane storm surge along the northern Gulf of Mexico. *J. Geophys. Res. Oceans* 121 (5), 3625–3658.
- Bilskie, M.V., Hagen, S.C., Medeiros, S.C., Passeri, D.L., 2014. Dynamics of sea level rise and coastal flooding on a changing landscape. *Geophys. Res. Lett.* 41 (3), 927–934.
- Blain, C.A., Westerink, J.J., Luettich, R.A., 1998. Grid convergence studies for the prediction of hurricane storm surge. *Int. J. Numer. Meth. Fluid.* 26 (4), 369–401.
- Blum, M.D., Roberts, H.H., 2009. Drowning of the Mississippi delta due to insufficient sediment supply and global sea-level rise. *Nat. Geosci.* 2 (7), 488–491.
- Blum, M.D., Roberts, H.H., 2012. The Mississippi delta region: past, present, and future. *Annu. Rev. Earth Planet. Sci.* 40 (1), 655–683.
- Brock, J., et al., 1999. Aircraft laser altimetry for coastal process studies. In: *Coastal Sediments '99: Proceedings of the 4th International Symposium on Coastal Engineering and Science of Coastal Sediment Processes*, pp. 2414–2429.
- Brock, J.C., Purkis, S.J., 2009. The emerging role of lidar remote sensing in coastal research and resource management. *J. Coast. Res.* SI (53), 1–5.
- Bunya, S., et al., 2010. A high-resolution coupled riverine flow, tide, wind, wind wave, and storm surge model for southern Louisiana and Mississippi. Part i: model development and validation. *Mon. Weather Rev.* 138 (2), 345–377.
- Campanella, R., 2008. *Bienville's Delimma: a Historical Geography of New Orleans*. University of Louisiana at Lafayette. Center for Louisiana Studies, Lafayette.
- Chen, Q., Wang, L., Tawes, R., 2008. Hydrodynamic response of northeastern gulf of Mexico to hurricanes. *Estuar. Coast* 31 (6), 1098–1116.
- Chen, Q., Zhao, H., 2011. Theoretical models for wave energy dissipation caused by vegetation. *J. Eng. Mech.* 138 (2), 221–229.
- Chen, Q., Zhao, H., Hu, K., Douglass, S.L., 2005. Prediction of wind waves in a shallow estuary. *J. Waterw. Port. Coast. Ocean Eng.* 131 (4), 137–148.
- Coastal Protection and Restoration Authority of Louisiana, 2017. In: Louisiana, C.P.R.A.o. (Ed.), *Louisiana's Comprehensive Master Plan for a Sustainable Coast*. Baton Rouge, LA.
- Cobell, Z., Zhao, H.H., Roberts, H.J., Clark, F.R., Zou, S., 2013. Surge and wave modeling for the Louisiana 2012 coastal master plan. *J. Coast. Res.* 67, 88–108.
- Coleman, J.M., Roberts, H.H., Stone, G.W., 1998. Mississippi river delta: an overview. *J. Coast. Res.* 699–716.
- Costanza, R., et al., 2008. The value of coastal wetlands for hurricane protection. *Ambio* 37 (4), 241–248.
- Couvillion, B.R., et al., 2011. In: US Department of the Interior, U.G.S. (Ed.), *Land Area Change in Coastal Louisiana (1932 to 2010)*, pp. 1–12.
- Cox, A.T., Greenwood, J.A., Cardone, V.J., Swail, V.R., 1995. An Interactive Objective Kinematic Analysis System, Alberta, Canada.
- Dietrich, J.C., et al., 2011. Performance of the unstructured-mesh, swanþ- adcirc model in computing hurricane waves and surge. *J. Sci. Comput.* 52 (2), 468–487.
- Dietrich, J.C., et al., 2010. Modeling hurricane waves and storm surge using integrallycoupled, scalable computations. *Coast. Eng.* 58, 45–65.
- Gagliano, S.M., Kwon, H.J., Van Beek, J.L., 1970. Deterioration and restoration of coastal wetlands. *Coast. Eng. Proc.* 1 (12).
- Gagliano, S.M., Light, P., Becker, R.E., 1971. Controlled Diversions in the mississippi River Delta System: an Approach to Environmental Management, in: *Hydrologic and Geologic Studies of Coastal Louisiana*. Louisiana State University, Baton Rouge.
- Galloway, W.E., 1975. Process framework for describing the morphologic and stratigraphic evolution of deltaic depositional systems. *Geol. Soc.* 87–98 (Deltas: Models for Exploration).
- Gould, H.R., McFarlan, E.J., 1959. Geologic history of the chenier plain, south-western Louisiana. *Trans. Gulf Coast Assoc. Geol. Soc.* 9, 261–270.
- Harrison, R., 2015. Impact of the Gulf Intracoastal Waterway (giww) on Freight Flows in the Texas-Louisiana Megaregion.
- Howe, H.W., Russell, R.J., McGuire, J.H., 1935. *Geology of Cameron and Vermillion Parishes; Physiography of Coastal Southwest Louisiana*, Baton Rouge, LA.
- Huh, O.K., Walker, N.D., Moeller, C., 2001. Sedimentation along the eastern chenier coast: down drift impact of a delta complex shift. *J. Coast. Res.* 17 (1), 72–81.
- Irish, J.L., Resio, D.T., Ratcliff, J.J., 2008. The influence of storm size on hurricane surge. *J. Phys. Oceanogr.* 38 (9), 2003–2013.
- Jevrejeva, S., Jackson, L.P., Riva, R.E., Grinsted, A., Moore, J.C., 2016. Coastal sea level rise with warming above 2 degrees c. *Proc. Natl. Acad. Sci. U. S. A.* 113 (47), 13342–13347.
- Karim, M.F., Mimura, N., 2008. Impacts of climate change and sea-level rise on cyclonic storm surge floods in Bangladesh. *Global Environ. Change* 18 (3), 490–500.
- Kashiyama, K., Saitoh, K., Gehr, M., Tezduyar, T.E., 1997. Parallel finite element nodes for large-scale computation of storm surges and tidal flows. *Int. J. Numer. Meth. Fluids.* 24 (12), 1371–1389.
- Kolar, R.L., Gray, W.G., Westerink, J.J., Luettich, R.A., 1994. Shallow water modeling in spherical coordinates: equation formulation, numerical implementation and application. *J. Hydraul. Res.* 32 (1), 3–24.
- Krabill, W.B., Collins, J.G., Link, L.E., Swift, R.N., Butler, M.L., 1984. Airborne laser topographic mapping results. *Photogramm. Eng. Rem. Sens.* 50 (6), 685–694.
- Lawler, S., Haddad, J., Ferreira, C.M., 2016. Sensitivity considerations and the impact of spatial scaling for storm surge modeling in wetlands of the mid-atlantic region. *Ocean Coast Manag.* 134, 226–238.
- Lesser, G.R., Roelvink, J.A., Van Kester, J.A.T.M., Stelling, G.S., 2004. Development and validation of a three-dimensional morphological model. *Coast. Eng. Proc.* 51 (8), 883–915.
- Loder, N.M., Irish, J.L., Cialone, M.A., Wamsley, T.V., 2009. Sensitivity of hurricane surge to morphological parameters of coastal wetlands. *Estuar. Coast. Shelf Sci.* 84 (4), 625–636.
- Lovelace, J.K., 1994. *Storm-tide Elevations Produced by Hurricane Andrew along the Louisiana Coast, August 25–27, 1992*. US Geological Survey Open File Report, Baton Rouge, LA.
- Luettich Jr., R.A., Westerink, J.J., Scheffner, N.W., 1992. Adcirc: an Advanced Three-dimensional Circulation Model for Shelves, Coasts and Estuaries. U.S. Army Corps of Engineers, ERDC-ITL-K, 3909 Halls Ferry Rd., Vicksburg, MS, 39180–6199.
- Luettich, R., Westerink, J., 2004. Formulation and Numerical Implementation of the 2d/ 3d Adcirc Finite Element Model Version 44.Xx, p. 74.
- Massey, T.C., Ratcliff, J.J., Cialone, M.A., 2015. North atlantic coast comprehensive study (naccs) storm simulation and statistical analysis: Part ii-high performance semiautomated production system. *Proc. Coast. Sediments 2015*.
- Massey, T.C., Wamsley, T.V., Cialone, M.A., 2011. Coastal storm modeling-system integration. *Solut. Coast. Disasters* 2011, 99–108.
- McGee, B.D., Goree, B.B., Tollett, R.W., Woodward, B.K., Kress, W.H., 2006. Hurricane Rita Surge Data, Southwestern Louisiana and Southeastern Texas, September–November 2005.
- Mederios, S.C., Ali, T., Hagen, S.C., Raiford, J.P., 2011. Development of a seamless topographic/bathymetric digital terrain model for tampa bay, Florida. *Photogramm. Eng. Rem. Sens.* 77 (12), 1249–1256.
- Merriam-Webster, 2017. Isopleth. *Merriam-Webster.com*.
- Moeller, C., et al., 2014. Wave attenuation over coastal salt marshes under storm surge conditions. *Nat. Geosci.* 7 (10), 727–731.
- Mori, N., et al., 2014. Local amplification of storm surge by super typhoon haiyan in leyte gulf. *Geophys. Res. Lett.* 41 (14), 5106–5113.
- National Oceanic and Atmospheric Administration, 2018. *Tides and Currents. Center for Operational Oceanographic Products and Services*.
- Parris, A., et al., 2012. *Global Sea Level Rise Scenarios for the Us National Climate Assessment Tech Memo Oar Cpo-1, p. 37*.
- Powell, M.D., Houston, S.H., Amat, L.R., Morisseau-Leroy, N., 1998. The hr3 real-time hurricane wind analysis system. *J. Wind Eng. Ind. Aerod.* 77–8 (78), 53–64.
- Resio, D.T., Westerink, J.J., 2008. Modeling the physics of storm surges. *Phys. Today* 61, 33–38.
- Restore the Mississippi Delta Coalition, 2012. In: *Special Engineering and Science Team (Ed.), Answering 10 Fundamental Questions about Restoring the mississippi Delta*.
- Roberts, H.H., 1997. Dynamic changes of the holocene Mississippi river delta plain: the delta cycle. *J. Coast. Res.* 13 (3), 605–627.
- Russell, R.J., Howe, H.V., 1935. Cheniers of southwestern Louisiana. *Geogr. Rev.* 25, 449–461.
- Sallenger Jr., A.H., et al., 1999. Recent el nino eroded u.s. West coast: a study conducted with the help of an airborne laser found that much of the u.s. West coast was altered due to effects of the 1997–1998 el nino. *Earth Space* 5–9.
- Sallenger Jr., A.H., et al., 2003. Evaluation of airborne topographic lidar for quantifying beach changes. *J. Coast. Res.* 19 (1), 125–133.
- Sallenger Jr., A.H., Wright, C.W., Lillycrop, W.J., 2007. Coastal-change impacts during hurricane katrina: an overview. In: *Coastal Sediments '07: Sixth International Symposium on Coastal Engineering and Science of Coastal Sediment Processes*. Proceedings. American Society of Civil Engineers, New Orleans, LA, pp. 888–896.

- Sanders, B.F., Schubert, J.E., Detwiler, R.L., 2010. Parbrezo: a parallel, unstructured grid, godunov-type, shallow-water code for high-resolution flood inundation modeling at the regional scale. *Adv. Water Resour.* 33 (12), 1456–1467.
- Sawyer, J.S., 1956. The vertical circulation at meteorological fronts and its relation to front genesis. *Proc. Roy. Soc. Lond. A: Math. Phys. Eng. Sci.* 234 (1198), 346–362.
- Seaber, P.R., Kapinos, F.P., Knapp, G.L., 1987. Hydrologic Unit Maps. US Government Printing Office, Washington (DC).
- Seaber, P.R., Kapinos, F.P., Shanton, S.A., 1975. Us geological survey state hydrologic units maps. *Geosci. Inf. Proc. Geosci. Inf. Soc.* 5, 41–53.
- Shepard, C.C., Crain, C.M., Beck, M.W., 2011. The protective role of coastal marshes: a systematic review and meta-analysis. *PLoS One* 6 (11) e27374.
- Stocker, T.F., et al., 2013. Climate Change 2013. The Physical Science Basis. Working Group I Contribution to the Fifth Assessment Report of the Intergovernmental Panel on Climate Change-abstract for Decision-makers. Groupe d'experts intergouvernemental sur l'évolution du climat/Intergovernmental Panel on Climate Change-IPCC. C/O World Meteorological Organization, 7bis Avenue de la Paix, CP2300 CH-1211 Geneva 2 (Switzerland).
- Suzuki, T., Zijlema, M., Burger, B., Meijer, M.C., Narayan, S., 2012. Wave dissipation by vegetation with layer schematization in swan. *Coast. Eng. Proc.* 59 (1), 64–71.
- Sweet, W.V., et al., 2017. Global and Regional Sea Level Rise Scenarios for the united states. National Oceanic and Atmospheric Administration, Silver Spring, Maryland.
- Twilley, R.R., et al., 2016. Co-evolution of wetland landscapes, flooding, and human settlement in the Mississippi river delta plain. *Sustain. Sci.* 1–21.
- U.S. Army Corps of Engineers, 1963. Interim Survey Report: Morgan City, Louisiana and Vicinity (No. Serial No. 63). New orleans, louisiana.
- U.S. Army Corps of Engineers, 2016. The mississippi River Drainage Basin. United States Geological Survey, 2015. Hydrologic Unit Maps.
- van Rijn, L.C., Walstra, D.J.R., van Ormondt, M., 2007. Unified view of sediment transport by currents and waves. Iv: application of morphodynamic model. *J. Hydraul. Eng.* 133 (7), 776–793.
- Walstra, D.J., et al., 2012. A comprehensive sediment budget for the Mississippi barrier islands. *Coast. Eng. Proc.* 1 (33), 81.
- Wamsley, T.V., Cialone, M.A., Smith, J.M., Atkinson, J.H., Rosati, J.D., 2010. The potential of wetlands in reducing storm surge. *Ocean Eng.* 37, 59–68.
- Westerink, J.J., et al., 2008. A basin- to channel-scale unstructured grid hurricane storm surge model applied to southern Louisiana. *Mon. Weather Rev.* 136 (3), 833–864.
- Zhang, K., et al., 2012. The role of mangroves in attenuating storm surges. *Estuar. Coast Shelf Sci.* 102, 11–23.